IEEE Access
Multidisciplinary | Rapid Review | Open Access Journal

Received 4 August 2023, accepted 17 August 2023, date of publication 21 August 2023, date of current version 28 August 2023.

Digital Object Identifier 10.1109/ACCESS.2023.3307016

APPLIED RESEARCH

Effect of Change of Reluctance Launcher Parameters on Projectile Velocity

VEKIL SARI
Electrical and Electronics Engineering Department, Sivas Cumhuriyet University, 58140 Sivas, Turkey
e-mail: vsari@cumhuriyet.edu.tr

ABSTRACT In this study, it is aimed to increase the projectile velocity by changing some parameters of the reluctance launcher. Studied parameters are the initial position of the projectile, the coating of the coil with ferrite, the coil length and the barrel outer diameter. A 3D Maxwell model of the reluctance launcher was generated to examine the effect of the change of these parameters on the projectile velocity. After the 3D model of the launcher was generated, analysis was done for each parameter. During the analysis for a parameter, the other parameters were kept constant. As a result of the analysis of the projectile position, it was determined that the projectile velocity is the highest when the projectile position is −2. It has been determined that the velocity of the projectile increases if the coil is coated with ferrite. It has been determined that the projectile velocity is the highest when the coil length is 7 cm. It has been determined that the highest projectile velocity is obtained when the barrel outer diameter is 18 mm. Using these results, the Maxwell model of the improved launcher was generated. The projectile velocity in the Maxwell model of the initial launcher is 19.24 m/sec. The projectile velocity of the improved launcher in the Maxwell model is 25.8 m/sec. By improving the launcher, a velocity increase of 34.09% was achieved. Later, this launcher was built and the parameters were investigated experimentally. In the experimental work, the projectile velocity of the initial launcher was measured as 19.11 m/sec, and the projectile velocity of the improved launcher was measured as 24.9 m/sec. As a result of the experimental work, a velocity increase of 30.29% was obtained by improving the launcher.

INDEX TERMS Coilgun, electromagnetic launching, linear accelerators, reluctance launchers.

I. INTRODUCTION

The velocity of the electromagnetic launchers is higher than the conventional launchers [1]. Therefore, number of the studies on electromagnetic launchers are increasing. Electromagnetic launchers can be classified into 6 categories: Indirect (IND), Direct (DIR), Electro-thermal-chemical (ETC), Magnetic (MAG), Electrostatic (EST) and Hybrid (HYB). Among these categories, the railguns and the coilguns are the most studied ones. Railgun is a Constant specific force (CSF) type of DIR category. The reluctance launchers which is a type of coilguns is a Variable specific force (VSF) of DIR category [2].

The railguns consist of two rails and a moving armature. When a current flows through the rails, a force is generated and causes the armature to move [3]. The object to be launched is placed in front of the armature, so that it can be launched. The projectile velocity of the railguns is high but the deformation and the friction losses are also high due to the high current flowing through the contacts [4], [5], [6]. The friction is low in reluctance launchers where there are no contacts. Reluctance launchers are used in many fields such as aviation, military, and hyper speed applications [7]. The reluctance launchers are structurally simple and easy to control [8], [9], [10]. When compared to a coilgun, a railgun has a higher projectile velocity, but the required current is very high. The railgun is used to launch larger masses, while the coilgun is used to launch smaller masses.

Reluctance launchers consist of a coil, a non-magnetic barrel and a ferromagnetic projectile to be launched. When the coil is energized, the induced magnetic field exerts a force that pulls the projectile towards the center of the coil.

The associate editor coordinating the review of this manuscript and approving it for publication was Wei Xu.

The energy must be shut down when the projectile reaches the center of the coil. Otherwise, the projectile will again be pulled back to the center of the coil [11]. This effect is called the suck-back effect [12], [13], [14], [15], [16]. It decreases the velocity of the projectile when it is out of the barrel. The coil energy must be shut down at the right time when the projectile reaches to the center of the coil. The energy on the coil must be immediately dampened. A capacitor was used in a previous study [14] for dampening the coil energy where a resistance was used in another study [17].

Electromagnetic launchers convert electromagnetic energy into mechanical energy [18]. The input is the electrical energy stored in the capacitor, and the output is the kinetic energy of the projectile. The efficiency of the electromagnetic launchers is given in Equation 1. Because all the energy in the capacitor is not used, the equation is transformed into Equation 2 when the remaining energy is subtracted [19].

$$Efficiency = \frac{Kinetic\ Energy\ of\ Projectile}{Electrical\ Energy\ of\ Capacitors} \quad (1)$$

$$\eta = \frac{mu_{exit}^2}{C\left(V_{before}^2 - V_{after}^2\right)} \quad (2)$$

Sensors should be used to shut down the energy at the right place. These sensors must be positioned as they will shut down the coil energy before the force on the projectile becomes negative. Furthermore, the projectile can also be used as a switch of the circuit that supplies energy to the coil. Thus, the contact points of the projectile can be adjusted and the coil can be energized or de-energized whenever necessary [20]. But, then there will be contact and friction.

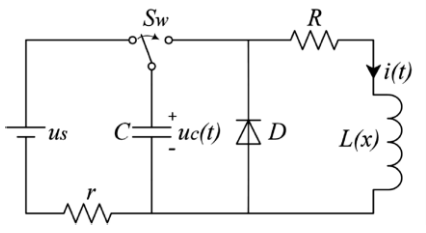

FIGURE 1. The equivalent circuit diagram of the reluctance launcher.

The equivalent circuit diagram of the reluctance launcher is given in Figure 1 [21]. Here, the capacitor is charged by the source voltage, then the switch position is changed and the energy at the capacitor is supplied to the coil. According to the reluctance theory, the magnetic field induced by the current flowing through the coil, pulls the projectile into the center of the coil. The force that pulls the projectile into the center of the coil is related with the mutual inductance of the coil [12], [13].

There have been many studies on increasing the projectile velocity by changing the parameters of the reluctance launchers. In such studies, switching of the energy applied on the coil [15], changing the material and geometry of the projectile [16], [22], [23], [24], [25], [26], changing the initial position of the projectile [7], [11], [27], and changing the geometry of the coil [8], [28] were also taken into consideration.

In this study, the 3D Maxwell model of the reluctance launcher was generated. Then the chosen parameters of the reluctance launcher (the initial position of the projectile, coating of the coil with ferrite, coil length and the barrel outer diameter) were changed and the change in the projectile velocity was investigated. At the end of these investigations, the values of the parameters that increase the projectile velocity were determined and the Maxwell model of the improved launcher was generated. Then, the reluctance launcher was built and used to compare the model and the experimental results.

II. MATERIAL AND METHOD

Before implementing electromagnetic systems, the model of the system is constructed using electromagnetic analysis software, and then information is gathered by analyzing this model. Using this collected information, the system can be optimized. The analysis of the reluctance launchers is complicated and difficult due to the non-linear B-H characteristics of the ferromagnetic projectile used in the reluctance launchers. Therefore, in the investigation of reluctance launchers, a software that uses finite elements analysis is utilized [14], [16], [17], [20], [21], [24], [25], [26], [28], [29], [30], [31], [32].

In a previous study [26], the 3D Maxwell model of the reluctance launcher was generated and the effect of the projectile material and geometry on the projectile velocity was investigated. AISI1020, AISI1050, and AISI12L14 were used as the projectile materials. It was determined that the velocity of the projectile constructed from AISI1050 material which has a higher magnetic permeability than the others, is higher than the other projectiles. Using a projectile of which geometry was not modified, a projectile velocity of 19.24 m/sec was obtained. To investigate the effect of the projectile geometry, empty projectiles and projectiles with notches were used. It was determined that the projectile velocity increases when the projectile is empty. Figure 2 and Table 1 show the dimensions of the launcher that was previously investigated.

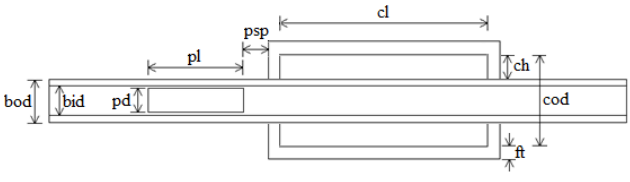

FIGURE 2. Dimensions of the previously investigated projectile.

In this study, the parameters affecting the projectile velocity were investigated and four parameters that we did not investigate in our previous studies were selected. These parameters are; the initial position of the projectile, coating of the projectile with ferrite, coil length and the barrel outer diameter.

TABLE 1. Dimensions of the previously investigated projectile.

Abbreviation	Description	Value
psp	Projectile starting position	0
bod	Barrel outer diameter	20 mm
bid	Barrel inner diameter	13 mm
pd	Projectile diameter	12,5 mm
pl	Projectile length	40 mm
cl	Coil length	80 mm
cod	Coil outer diameter	30 mm
ch	Coil height	5 mm
ft	Ferrite thickness	0
N	Number of coil turns	540 turns

The effect of change of these parameters on the projectile velocity were investigated using the 3D Maxwell model of the reluctance launcher.

TABLE 2. Chemical combination ratios of AISI1050 material.

	Chemical content (%)				
Code	C	Si	Mn	Pmax	Smax
1050	0.50-0.57	0.15-0.35	0.40-0.70	0.025	0.035

TABLE 3. AISI1050 material in the standards of other countries.

Germany DIN 17210		France	UK	Italy	Japan	CIS	USA
Material no.	Symbol	AFNOR	B.S.	UNI	JIS	GOST	AISI /SAE
1.123	Cf53	XC 48 H1 TS	060 A52; 070 M 55	C 53	S50 C	50	1050

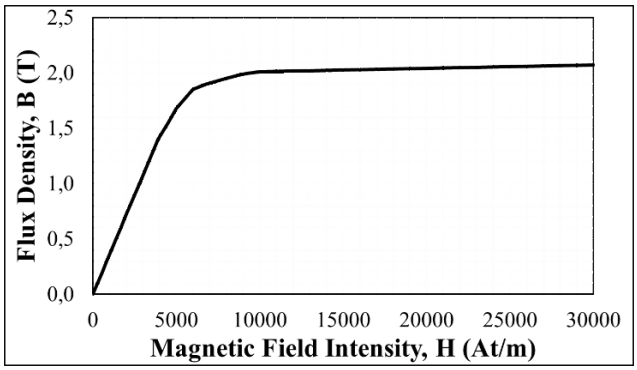

FIGURE 3. B-H curve for AISI1050.

In a previous study [26], the highest velocity (19.24 m/sec) was obtained with the projectile that was constructed using AISI1050 material (projectile geometry was kept constant). Therefore, projectiles constructed with AISI1050 material were used in this study. AISI1050 material is known as the production steel in the industry. Steels are entitled according to the carbon rate in their structure. 1050 steel contains 0.50% carbon in it, thus called as 1050. Table 2 shows the chemical combination ratios of the AISI1050 material and Table 3 shows the codes of the AISI1050 material in other countries. Figure 3 shows the B-H characteristics of the AISI1050 material [25].

In this study, the effect of each parameter on the projectile velocity was investigated. In order to prevent the effect of other parameters on the projectile velocity, other parameters were kept constant by taking the values in Table 1.

A. EFFECT OF THE PROJECTILE'S INITIAL POSITION ON THE PROJECTILE VELOCITY

The inductance of the coil can be found by dividing the flux linkage into the current as given in Equation 3. Here $\psi(x)$ is flux linkage, which changes depending on the position of the projectile, $L(x)$ is the coil inductance that changes depending on the position of the projectile [21].

$$L(x) = \frac{\psi(x)}{i} \tag{3}$$

In the electromagnetic launcher, the force applied to the projectile is proportional to the derivative of the coil inductance [33]. The inductance of the coil changes depending on the position of the projectile [34]. Therefore, the initial position of the projectile affects the force applied to the projectile and the projectile velocity. Equation 4 shows that the force applied to the projectile is proportional to the derivative of the coil inductance [21]. Figure 4 shows the variation of flux linkage with respect to position, Figure 5 shows the change of coil inductance, and Figure 6 shows the variation of the derivative of the inductance.

$$F = \frac{i^2}{2}\frac{dL(x)}{dx} \tag{4}$$

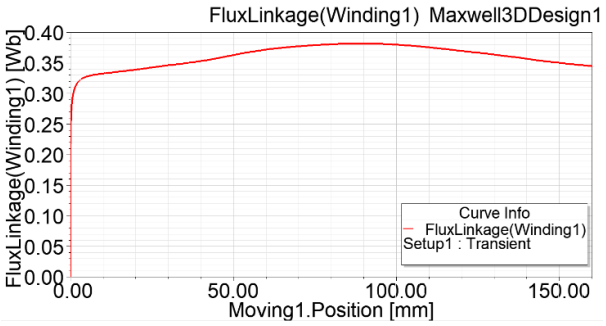

FIGURE 4. Flux linkage vs position.

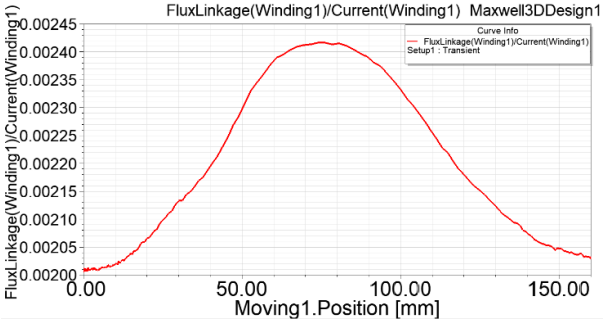

FIGURE 5. Inductance (ψ(x) /i) vs position.

In this study, the effect of the projectile's initial position was investigated first. As shown in Figure 7, position is

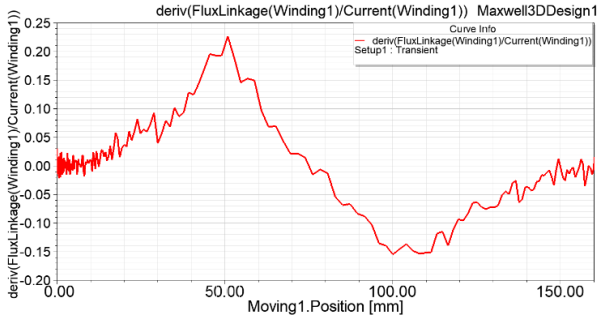

FIGURE 6. Derivative of inductance vs position.

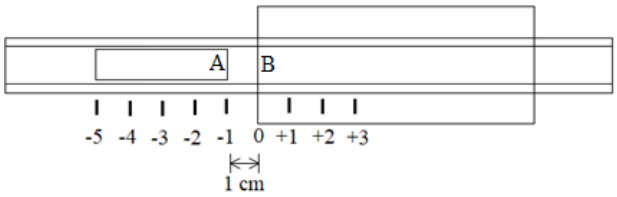

FIGURE 7. Initial positions of the projectile.

assumed 0 when the point A of the projectile is aligned with the point B of the coil. The position is −1 when the projectile is 1 cm away from the coil, and the position is +1 when the projectile is 1 cm inside the coil. Figure 7 shows the initial positions of the projectile. In Figure 7, the projectile is at position −1 initially.

Using the generated Maxwell model, the projectile velocities were obtained for different initial positions. Figure 8 and Table 4 shows the projectile velocities according to the initial positions of the projectile. Other parameters of the launcher were kept constant (The values in Table 1 were taken) while obtaining these results. Results show that, the projectile velocity is higher when the projectile position is −2 initially. In this case, the velocity is 22.35 m/sec. There is a 16.16% increase in the projectile velocity when it is launched from position −2 instead of position 0.

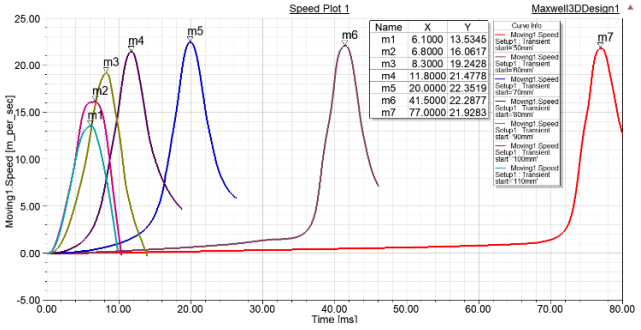

FIGURE 8. Projectile velocities vs the initial position of the projectile.

B. EFFECT OF COATING THE COIL WITH FERRITE ON PROJECTILE VELOCITY

As the second parameter, coating the coil with ferrite was taken into account. The projectile velocities were obtained by coating the coil with ferrite which is 1-10 mm thick in the 3D Maxwell model. Figure 9 shows the velocity graphs vs the ferrite thickness. Table 5 and Figure 10 show that the projectile velocity increases when the projectile is coated with ferrite. On the other hand, Figure 10 shows velocity does not increase so much after 5 mm. Other parameters were kept constant to investigate the effect of ferrite thickness on velocity only (The values in Table 1 were taken). The projectile is at position 0 and 200 V is applied to the coil while obtaining these results. When the coil is coated with a 5-mm ferrite, the projectile velocity is 23.01 m/sec which corresponds to 19.59% increase compared to a non-coated coil.

TABLE 4. Projectile velocities vs the initial position of the projectile.

Initial position of projectile	Projectile velocity (m/sec)
-4	21.92
-3	22.28
-2	22.35
-1	21.47
0	19.24
+1	16.06
+2	13.53

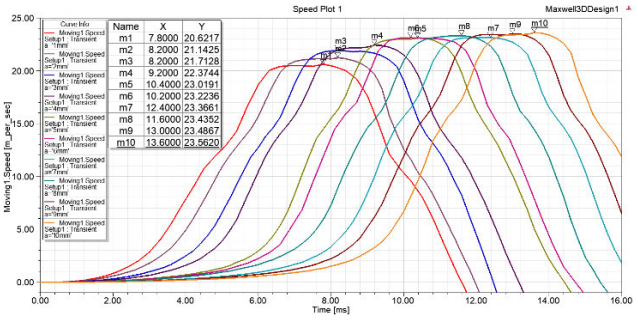

FIGURE 9. Projectile velocity vs ferrite thickness.

TABLE 5. Projectile velocities when the coil Is coated with ferrite.

Ferrite Thickness (mm)	Projectile velocity (m/sec)
0	19.24
1	20.62
2	21.14
3	21.71
4	22.37
5	23.01
6	23.22
7	23.36
8	23.43
9	23.48
10	23.56

When ferrite is coated around the coil, it does not allow the magnetic field to move away from the coil, since ferrite is a ferromagnetic material and its permeability is higher than air. Since the magnetic field does not move far from the coil, it will be more intense and will affect the projectile more. As a result, the projectile velocity will increase.

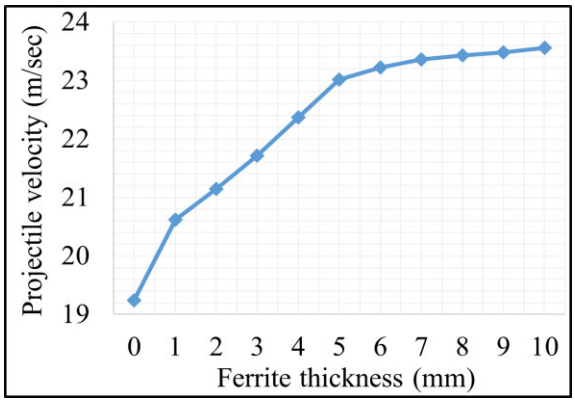

FIGURE 10. Projectile velocity vs ferrite thickness.

C. EFFECT OF CHANGE OF COIL LENGTH ON PROJECTILE VELOCITY

In electromagnetic launchers, the electromagnetic force applied to the projectile determines the projectile velocity. The more electromagnetic force applied to the projectile, the faster the projectile will be launched. Another parameter that can increase the projectile velocity is the coil length. Therefore, coil length was chosen as the third parameter. The relationship between projectile velocity and coil length is given in Equation 5 [20].

$$F_m = Ci^2\left(\frac{l-x_1}{\sqrt{(l-x_1)^2+R^2}}+\frac{x_1}{\sqrt{x_1^2+R^2}}\right)^2 - Ci^2\left(\frac{l-x_2}{\sqrt{(l-x_2)^2+R^2}}+\frac{x_2}{\sqrt{x_2^2+R^2}}\right)^2 \quad (5)$$

where l is the length of the coil, i is current of the coil, x is relative position, R is the radius of the coil, and C is a constant. The value of constant C is given in Equation 6.

$$C = \frac{1}{8}(\mu-\mu_0)AN^2 \quad (6)$$

where N is the number of turns per unit length, μ is permeability of the medium, A is the cross-sectional area where the magnetic flux passes vertically (m^2).

The number of turns (N) was kept constant (540-turn) and the coil length was changed between 40-100 mm. Figure 11 and Table 6 shows the projectile velocities obtained by changing the coil lengths. The results show that the projectile has the highest velocity when the coil length is 70 mm. The projectile is at position 0 and 200 V is applied to the coil while obtaining these results. When the coil length is 70 mm, the projectile velocity is 21.03 m/sec which corresponds to 9.3% increase compared to a 80 mm (initial value) coil.

The relationship between coil length and projectile velocity is as follows: A coil with a fixed number of turns does not have enough distance to accelerate the projectile when its size is small. As the coil length increases, there is a distance inside the projectile that allows it to move and increase its velocity. Then, as the coil length increases, the magnetic field intensity will decrease (since the number of turns is constant), and the projectile velocity decreases after a certain length.

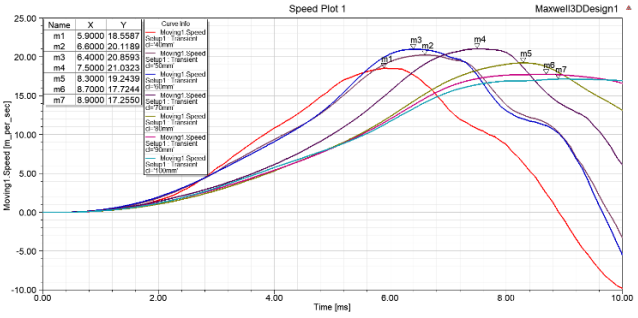

FIGURE 11. Projectile velocity vs the coil length.

TABLE 6. Projectile velocity vs coil length.

Coil length (mm)	Projectile velocity (m/sec)
40	18.55
50	20.11
60	20.85
70	21.03
80	19.24
90	17.72
100	17.25

D. EFFECT OF CHANGE OF BARREL OUTER DIAMETER ON PROJECTILE VELOCITY

As seen in Equation 5, the electromagnetic force applied to the projectile also depends on the radius of the coil. The radius of the coil is the same as the outer radius of the barrel. Therefore, barrel outer diameter was taken into account as the fourth parameter. The change of the projectile velocity was investigated by changing the barrel outer diameter between 15-23 mm. The number of turns was kept constant (540-turn). Figure 12 and Table 7 shows the projectile velocities with different barrel outer diameters. The projectile velocity is 20.3 m/sec when the barrel outer diameter is 18 mm which corresponds to a 5.5% increase in the projectile velocity in comparison with a 20-mm barrel outer diameter.

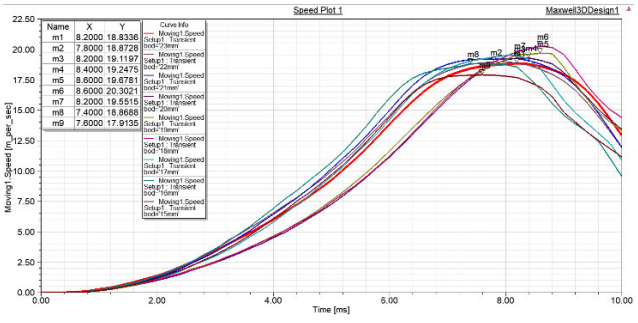

FIGURE 12. Projectile velocity vs barrel outer diameter.

TABLE 7. Projectile velocity vs Barrel outer diameter.

Barrel Outer Diameter (mm)	Projectile velocity (m/sec)
23	18.83
22	18.87
21	19.11
20	19.24
19	19.67
18	20.30
17	19.55
16	18.86
15	17.91

The effect of the change in the barrel outer diameter on the projectile velocity was investigated while the inner diameter of the barrel was constant. While the inner diameter of the barrel is constant, the change in the outer diameter of the barrel (barrel wall thickness) affects the distance between the coil and the projectile, thus the coupling. When the barrel outer diameter is very small, the coil is close to the projectile, as the barrel outer diameter increases, the coil moves away from the projectile. It affects the most at a certain value. As the barrel outer diameter increases, the projectile launch velocity increases up to a certain value, then decreases.

E. IMPROVED LAUNCHER

The Maxwell model of the improved launcher was generated using the values of four parameters that maximize the projectile velocity. These values are: projectile initial position $= -2$, ferrite thickness $= 5$ mm, coil length $= 70$ mm and barrel outer diameter $= 18$ mm. New dimensions of the launcher are given in Figure 13 and Table 8. The projectile velocity of this launcher is 25.8 m/sec. When it is compared with the velocity of the initial launcher (19.24 m/sec) it corresponds to a 34.09% increase in the projectile velocity.

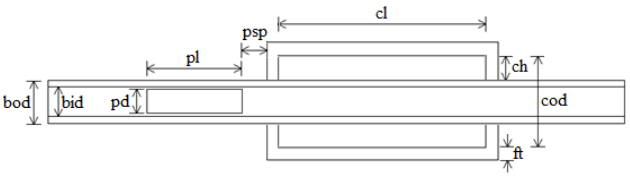

FIGURE 13. Dimensions of the improved launcher.

Figure 14 shows the projectile velocity graph of the improved launcher. The projectile velocity is 25.8 m/sec at 41.8 milliseconds. Figure 15 shows the magnetic flux density of the improved launcher at 41.8 milliseconds.

The force exerted by the reluctance launcher on the projectile can be derived from classical electromagnetic field theory. The force exerted to the projectile can be calculated according to Equation 7 [35].

$$F = \frac{1}{2} X \mu_0 \left(\frac{NI}{l}\right)^2 A \tag{7}$$

TABLE 8. Dimensions of the improved launcher.

Abbreviation	Description	Value
psp	Projectile starting position	-2
bod	Barrel outer diameter	18 mm
bid	Barrel inner diameter	13 mm
pd	Projectile diameter	12,5 mm
pl	Projectile length	40 mm
cl	Coil length	70 mm
cod	Coil outer diameter	30 mm
ch	Coil Height	6 mm
ft	Ferrite Thickness	5
N	Number of coil turns	540 turns

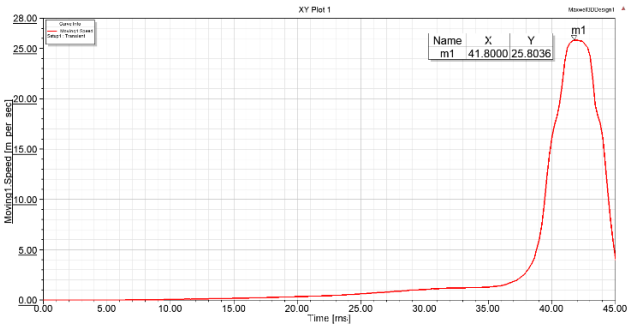

FIGURE 14. Projectile velocity graph of the improved launcher.

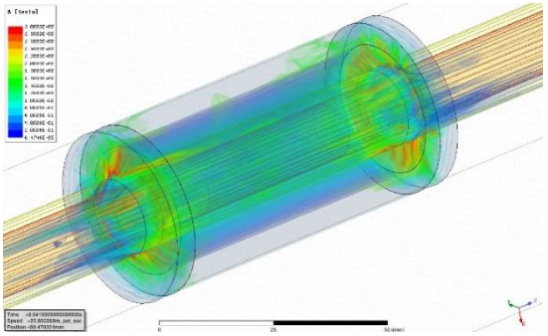

FIGURE 15. Magnetic flux density of the improved launcher at 41.8 milliseconds.

where

$$X = \frac{\mu}{\mu_0} - 1$$

$N =$ number of coil turns

$I =$ current flowing through the winding

$l =$ coil length

$A =$ coil cross-section area

At the end of the calculations, it was determined that Equation 7 did not give correct results. One of the reasons for this is leakage flux. Another reason is applying linear analysis to a nonlinear problem. The third reason is that the electromagnetic launch velocity is higher than the mechanical motion, and the mechanical transition process and the electromagnetic transition process are coupled and therefore cannot be considered separately. Due to the complexity of the

dynamic process, it is difficult to reach the solution using the analytic method. Reluctance launchers are designed using the finite element method (FEM) [35].

III. EXPERIMENTAL WORK

For the experimental work, the coil of the launcher was built using a 540-turn, 0.8 mm^2 cross-sectional cable. 4 pairs of TCST2300 optical sensors were used to detect the projectile. The resistance of the coil conductor is 1.2 ohm and its inductance is 1.5 mH. The first three of these sensor pairs were placed with 2 cm intervals. The position of the fourth optical sensor depends on the coil length. Positions of sensor pairs are shown in Figure 16. The velocity of the launched projectile must be measured correctly to be able to determine the performance of the launcher. Two pairs of TCST2300 sensors were placed on the barrel with 20 cm intervals to measure the projectile velocity. These sensor pairs are also shown in Figure 16. The time that takes the projectile to pass through these two sensor pairs is measured using PIC16F876 microprocessor and the projectile velocity is calculated by dividing the distance between sensors (20 cm) to time.

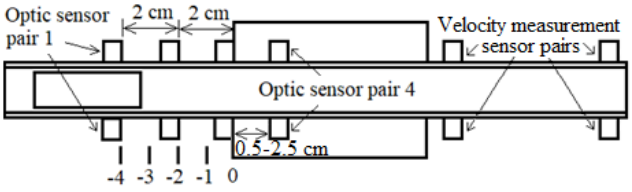

FIGURE 16. Positioning of sensor pairs.

Figure 17 shows the circuit schema of the launcher. IRG4PH50S was used as the IGBT in this circuit. For the IGBT to not to be harmed in case of conduction and blocking, D2, C3 and R16 were used as snubbers [36]. IGBTs should be isolated from the source. Because the voltage is relatively low between G-E and relatively high between C-E. Therefore, IGBT driver should be used [37]. IR2113 was used as the IGBT driver.

When there is no projectile at the barrel, the transmitters of all the optical sensor pairs are able to transmit light to the receivers and the outputs of the sensors are 0 V. Bases of T1-T4 transistors are at 0 potential which means that they are in blocking state. The HIN input of the driver is at 0 potential, thus HO is also at 0 potential and IGBT is not triggered. When the projectile is placed at the input of the barrel, the transmitter-receiver path of at least one of the optical sensors is interrupted. Assume that the projectile is placed in between the transmitter and receiver of optical sensor pair 1. In this case, the light does not reach the receiver of the optical sensor pair 1 and the supply voltage at the sensor output is applied to the base of transistor T1. T1 switches to conducting state and the supply voltage is applied to HIN. A trigger signal is sent to the IGBT from the HO output. Thus, capacitors which were charged with 200 V DC voltage are discharged through the coil. The magnetic field induced by the coil pulls

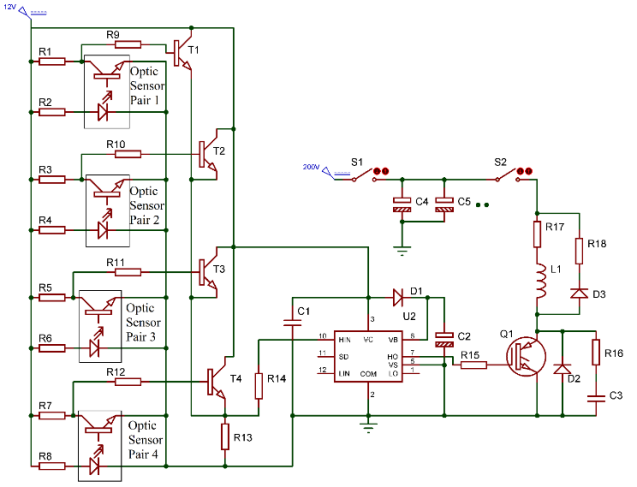

FIGURE 17. Circuit schema of the launcher.

the projectile into the center of the coil. IGBT is in conducting state while the projectile is between these four optical sensor pairs.

When the projectile is out of the optical sensor pairs, the receivers of all the sensor pairs are in conducting state. T1-T4 is in blocking state. HIN input is at 0 potential. HO output becomes 0 and IGBT switches to blocking state. No energy is applied to the coil. A diode (D3) and a resistor (R18) is connected in parallel to the coil to dampen the inductive current on the coil. Here, the position of the optical sensor pair 4 is important. It should be placed as the projectile will be at the middle of the coil when it is out of this sensor. In this study, the length of the projectile is constant (4 cm) but the length of the coil changes. As an example, when the coil is 8 cm, the 4th optical sensor pair is placed 2 cm inside the coil. When the coil length is 7 cm, it is placed 1.5 cm inside the coil. Thus, the projectile is always at the middle of the coil when it is out of the 4th optical sensor pair and the coil's energy is shut down.

S1 switch is closed when S2 switch is open and 8 capacitors of 2700 μF (a total of 21.6 mF) are charged by 200 V DC voltage. Then S1 is opened and S2 is closed and the energy stored in the capacitors is discharged over the coil. Resistor R17 shown in the schema in Figure 17 is the self-resistance of the coil. Diode D3 and the resistor R18 are used to dampen the energy on the coil when it is deenergized.

During the experimental work, the initial launcher was first built using the values given in Table 1. The projectile velocity of this launcher was measured as 19.11 m/sec. Figure 18 shows the initial launcher. Here, control, power and speed measurement sections are visible.

Then, the initial position of the projectile was studied as the first parameter and the effect of this parameter on the projectile velocity was investigated. Results are given in Table 9.

Coating of the coil with ferrite was studied as the second parameter and velocities were measured for this parameter. Investigation using Maxwell model showed that velocity

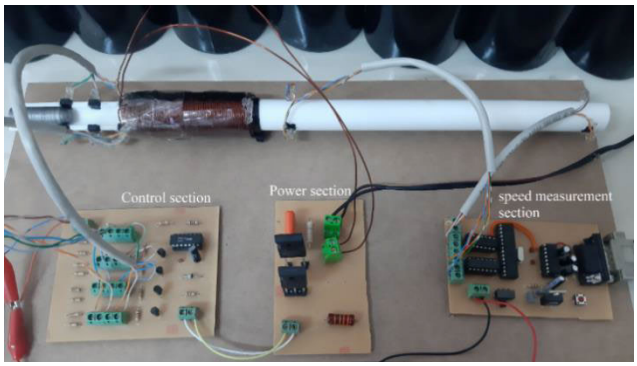

FIGURE 18. Initial launcher.

TABLE 9. Projectile velocity vs the initial position of the projectile.

Initial position of projectile	Projectile velocity (m/sec)
-3	21.75
-2	21.98
-1	21.85
0	19.11
+1	15.23

increase is negligible after ferrite thickness is 5 mm. Therefore, investigation was done up to 5 mm ferrite thickness. Projectile velocities,when the coil is coated with ferrite, is given in Table 10.

The coil length was studied as the third parameter. Here, the number of turns was kept constant. 5 different coils with 50 to 90 mm length were built and projectile velocities were measured in each case. Results are given in Table 11. Here, the position of the fourth optical sensor pair changes with the coil length. The distance of optical sensor pair 4 from the position 0 to the inside of the coil is shown in Figure 19 and the values are given in Table 11.

TABLE 10. Projectile velocities when the coil Is coated with ferrite.

Ferrite Thickness (mm)	Projectile velocity (m/sec)
0	19.11
1	20.38
2	21.36
3	21.79
4	22.25
5	22.64

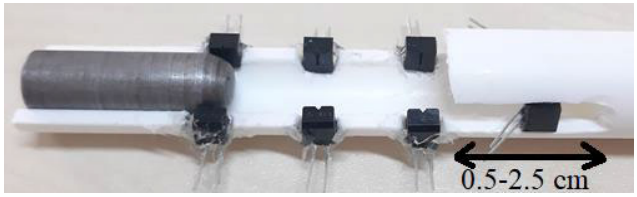

FIGURE 19. Sensor positions.

Finally, the projectile velocities were measured by changing the barrel outer diameter. Table 7 shows that the velocity

TABLE 11. Projectile velocity vs coil length.

Coil length (mm)	Projectile velocity (m/sec)	Position of optical sensor pair 4 (cm)
50	19.78	0.5
60	20.45	1
70	20.76	1.5
80	19.11	2
90	17.83	2.5

decreases when the barrel outer diameter is higher than 20 mm. Therefore the barrel outer diameter was changed between 16 mm - 20 mm in the experimental work. Measured velocities are given in Table 12.

TABLE 12. Projectile velocity vs barrel outer diameter.

Barrel outer diameter (mm)	Projectile velocity (m/sec)
20	19.11
19	19.35
18	20.14
17	19.28
16	18.55

After the effect of 4 parameters on the velocity was investigated, the improved launcher was built using these values. Initial projectile position is −2, ferrite thickness is 5 mm, coil length is 70 mm and the barrel outer diameter is 18 mm. Other parameters were kept constant (barrel inner diameter=13 mm, projectile diameter=12.5 mm, projectile length=40 mm, coil outer diameter=30 mm, coil height=6 mm, number of coil turns=540 turns). The projectile velocity was measured as 24.9 m/sec when it was launched with the improved launcher.

IV. RESULTS AND DISCUSSION

The initial position of the projectile was considered as the first parameter. 3D Maxwell model of the reluctance launcher was generated and the effect of initial position of the projectile on the projectile velocity was investigated using this model. The projectile velocity is the highest when the projectile is at position −2. The highest velocity is 22.35 m/sec and there is a 16.16% increase in comparison with the 0 position. In the experimental work, the projectile velocity was measured as 21.98 m/sec when the projectile was at position −2. There is a 1.68% error between the model and the experimental work. Figure 20 shows the comparison of results obtained using Maxwell model and experimental work.

The second parameter was the coating of the coil with ferrite. Projectile velocity increase when the coil is coated with ferrite. Velocity does not increase dramatically after the ferrite thickness is 5 mm. Therefore, only the case when the coil is coated with a 5-mm ferrite was investigated using the 3D Maxwell model. In this case, the projectile velocity is 23.01 m/sec which corresponds to a 19.59% increase. Figure 21 shows the comparison of projectile velocities when the coil is coated with ferrite.

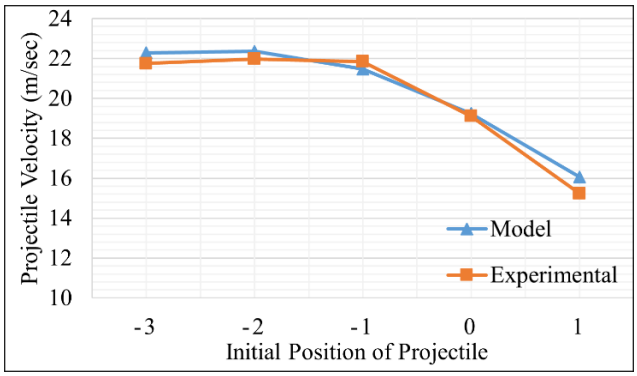

FIGURE 20. Comparison of velocity results in terms of initial position of projectile.

The third parameter was coil length and using the 3D Maxwell model; the highest projectile velocity was obtained (21.03 m/sec) when the coil length is 70 mm. It corresponds to a 9.3% increase (19.24 m/sec) compared to a 80 mm coil. The projectile velocity was measured as 20.76 m/sec in the experimental work when the coil length is 70 mm. There is a 1.3 % error between model and the experimental work. Figure 22 shows the comparison of the velocities by changing the coil lengths.

The fourth and the final parameter is the barrel outer diameter. Using the 3D Maxwell model, the highest velocity (20.3 m/sec) was obtained when the barrel outer diameter is 18 mm. Increase in the velocity versus a launcher with a 20 mm barrel outer diameter is 5.5% (19.24 m/sec). In the experimental work, the projectile velocity was measured as 20.14 m/sec when the barrel outer diameter is 18 mm. There is a 0.79% error between the model and the experimental work. Figure 23 shows the comparison of velocities when the barrel outer diameters are changed.

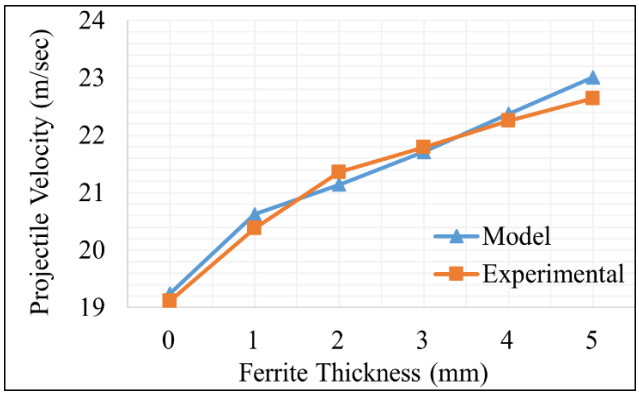

FIGURE 21. Comparison of velocities when the coil is coated with ferrite.

The reluctance launcher system was also investigated in terms of efficiency. The voltage applied to the launcher is 200 V. There is an approximately 50 V of decrease in the voltage after the launch. Thus, Vbefore is 200 V, and Vafter is 150 V while calculating the efficiency (Equation 2) for

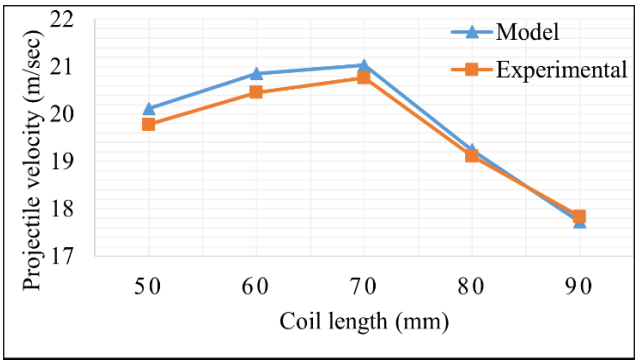

FIGURE 22. Comparison of velocities by changing coil length.

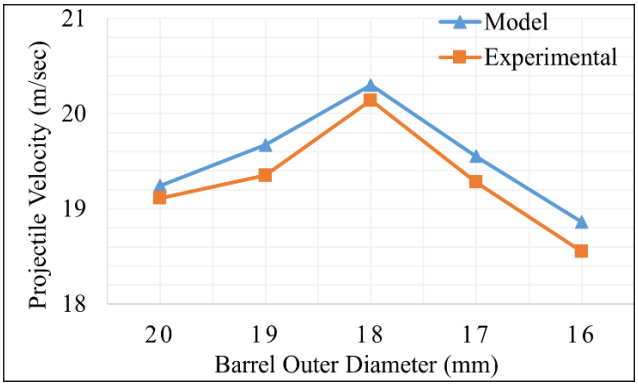

FIGURE 23. Comparison of velocity results when the barrel outer diameter changes.

all launch trials. The weight of the projectile is 36 grams. According to the results obtained from the model, the efficiency of the initial launcher is 3.5% and the efficiency of the improved launcher is 6.3%. According to the results obtained from the experimental work, the efficiency of the initial launcher is 3.47% and the efficiency of the improved launcher is 5.9%. After the improvement, there is a 2.8%, and a 2.33% increase in the efficiency according to the results obtained from the model and the experimental work respectively. These values are given in Table 13.

TABLE 13. Velocity and efficiency values for the improved launcher.

	Velocity before improvement (m/sec)	Efficiency before improvement (%)	Velocity after improvement (m/sec)	Efficiency after improvement (%)	Velocity increase rate (%)	Efficiency increase rate
Model	19.24	3.5	25.8	6.33	34.09	2.83
Experimental	19.11	3.47	24.9	5.9	30.29	2.43

V. CONCLUSION

In this study, it is aimed to increase the projectile velocity by changing four different parameters (initial position of the projectile, coating of the coil with ferrite, coil length,

and outer barrel diameter) of the reluctance launcher for which the projectile geometry was investigated previously. Therefore, 3D Maxwell model of the reluctance launcher was generated and the effect of these four parameters on the projectile velocity was investigated using Maxwell model. As a result of this investigation, for each parameter, the parameter values that provide the highest projectile velocity were determined. Then, 3D Maxwell model of the improved launcher was generated using these values. The projectile velocity before the improvement of these four launcher parameters is 19.24 m/sec. The velocity obtained after the improvement is 25.8 m/sec. By improving these four parameters there was a 34.09% increase in the velocity. Then the launcher was built and the parameters that were investigated using Maxwell model, were also investigated experimentally. The velocity of the initial launcher was measured as 19.11 m/sec and the velocity of the improved launcher was measured as 24.9 m/sec. As a result of the experimental work, there was a 30.29% increase in the velocity by improving the launcher. There is a 3.61% error between the model and the experimental work.

In this study, four parameters of the electromagnetic launcher were optimized and as a result of this optimization, the muzzle velocity was increased. As a result of optimizing these four parameters, a velocity close to the theoretical velocity was obtained. Because the Maxwell program gives results close to the theoretical results as in previous studies. Electromagnetic launchers have many parameters related to projectile, muzzle and coil. To achieve the fully optimized theoretical velocity of the electromagnetic launcher, all its parameters need to be optimized.

REFERENCES

[1] G. X. Cun, S. Wang, D. Guo, S. Guan, B. Liu, and B. Wu, "Design and implementation of a high-speed real-time position detection system in electromagnetic coil launcher," *IEEE Trans. Plasma Sci.*, vol. 48, no. 9, pp. 3203–3210, Sep. 2020, doi: 10.1109/TPS.2020.3019045.

[2] T. G. Engel, "Scientific classification method for electromagnetic launchers," *IEEE Trans. Plasma Sci.*, vol. 45, no. 7, pp. 1333–1338, Jul. 2017, doi: 10.1109/TPS.2017.2705177.

[3] H. Polat, N. Tosun, D. Ceylan, and O. Keysan, "Optimization of a convex rail design for electromagnetic launchers," *IEEE Trans. Plasma Sci.*, vol. 48, no. 6, pp. 2266–2273, Jun. 2020, doi: 10.1109/TPS.2020.2993785.

[4] L. Mascolo and A. Stoica, "Electro-magnetic launchers on the moon: A feasibility study," in *Proc. NASA/ESA Conf. Adapt. Hardw. Syst. (AHS)*, Edinburgh, U.K., Aug. 2018, pp. 37–42.

[5] Y. Zhu, Y. Wang, Z. Yan, L. Dong, X. Xie, and H. Li, "Multipole field electromagnetic launcher," *IEEE Trans. Magn.*, vol. 46, no. 7, pp. 2622–2627, Jul. 2010, doi: 10.1109/TMAG.2010.2044416.

[6] Y. Orbach, M. Oren, and M. Einat, "75 m/s simulation and experiment of two-stage reluctance coilgun," *J. Mech. Sci. Technol.*, vol. 36, no. 3, pp. 1123–1130, Mar. 2022, doi: 10.1007/s12206-022-0205-8.

[7] J. L. Rivas-Camacho, M. Ponce-Silva, and V. H. Olivares-Peregrino, "Experimental results concerning to the effects of the initial position of the projectile on the conversion efficiency of a reluctance accelerator," in *Proc. 13th Int. Conf. Power Electron. (CIEP)*, Guanajuato, Mexico, Jun. 2016, pp. 92–97, doi: 10.1109/CIEP.2016.7530737.

[8] H. Chen, R. Nie, and H. Wang, "A transverse flux single-phase tubular-switched reluctance linear launcher with eight-pole structure," *IEEE Trans. Plasma Sci.*, vol. 47, no. 5, pp. 2331–2338, May 2019, doi: 10.1109/TPS.2019.2900066.

[9] J. L. Rivas-Camacho, M. Ponce-Silva, and V. H. Olivares-Peregrino, "The ringer as an inductive power source for a reluctance accelerator," *IEEE Trans. Plasma Sci.*, vol. 47, no. 5, pp. 2275–2281, May 2019, doi: 10.1109/TPS.2019.2899103.

[10] G. Zhu, H. Hu, W. Guo, K. Zhang, Y. Chen, and X. Chen, "Magnetic force calculation in reluctance force launcher," *IEEE Trans. Magn.*, vol. 58, no. 6, pp. 1–9, Jun. 2022, doi: 10.1109/TMAG.2022.3167118.

[11] Y. Orbach, M. Oren, A. Golan, and M. Einat, "Reluctance launcher coil-gun simulations and experiment," *IEEE Trans. Plasma Sci.*, vol. 47, no. 2, pp. 1358–1363, Feb. 2019, doi: 10.1109/TPS.2018.2885710.

[12] S. Santosh Reelkar, "Electromagnetic launcher: Review of various structures," *Int. J. Eng. Res.*, vol. 9, no. 9, pp. 505–508, Sep. 2020, doi: 10.17577/IJERTV9IS090223.

[13] M. U. Manzoor, H. Asif, and T. Abbas, "Split coil based design of a coilgun," in *Proc. 13th Int. Conf. Emerg. Technol. (ICET)*, Islamabad, Pakistan, Dec. 2017, pp. 1–6, doi: 10.1109/ICET.2017.8281739.

[14] H.-M. Deng, Y. Wang, F.-L. Lu, and Z.-M. Yan, "Optimization of reluctance accelerator efficiency by an improved discharging circuit," *Defence Technol.*, vol. 16, no. 3, pp. 662–667, Jun. 2020, doi: 10.1016/j.dt.2019.08.013.

[15] A. Hassannia and K. Abedi, "Optimal switching scheme for multi-stage reluctance coilgun," *IEEE Trans. Plasma Sci.*, vol. 49, no. 3, pp. 1241–1246, Mar. 2021, doi: 10.1109/TPS.2021.3061299.

[16] H.-M. Deng, Y. Wang, and Z.-M. Yan, "Study on the influence of armature on the efficiency of reluctance accelerator," *Defence Technol.*, vol. 18, no. 2, pp. 293–304, Feb. 2022, doi: 10.1016/j.dt.2021.01.003.

[17] C. Liang, H. Xiang, X. Yuan, Z. Qiao, and Q.-A. Lv, "Reverse force suppression method of reluctance coil launcher based on consumption resistor," *IEEE Access*, vol. 9, pp. 62770–62778, 2021, doi: 10.1109/ACCESS.2021.3073905.

[18] W. Ying, R. A. Marshall, and C. Shukang, *Physics of Electric Launch*. Beijing, China: Science Press, 2004.

[19] G. W. Slade, "A simple unified physical model for a reluctance accelerator," *IEEE Trans. Magn.*, vol. 41, no. 11, pp. 4270–4276, Nov. 2005, doi: 10.1109/TMAG.2005.856320.

[20] B. Zhu, J. Lu, J. Wang, and S. Xiong, "A compulsator driven reluctance coilgun-type electromagnetic launcher," *IEEE Trans. Plasma Sci.*, vol. 45, no. 9, pp. 2511–2518, Sep. 2017, doi: 10.1109/TPS.2017.2731624.

[21] M. Lu, J. Zhang, X. Yi, and Z. Zhuang, "Advanced mathematical calculation model of single-stage RCG," *IEEE Trans. Plasma Sci.*, vol. 50, no. 4, pp. 1026–1031, Apr. 2022, doi: 10.1109/TPS.2022.3159533.

[22] H. Xiang, B. Lei, Z. Li, and K. Zhao, "Design and experiment of reluctance electromagnetic launcher with new-style armature," *IEEE Trans. Plasma Sci.*, vol. 41, no. 5, pp. 1066–1069, May 2013, doi: 10.1109/TPS.2013.2245151.

[23] F. Daldaban and V. Sari, "Design and implementation of a three-coil linear reluctance launcher," in *Proc. 16th Int. Power Electron. Motion Control Conf. Exposit.*, Antalya, Turkey, Sep. 2014, pp. 1084–1088, doi: 10.1109/EPEPEMC.2014.6980653.

[24] F. Daldaban and V. Sari, "Analysis of a reluctance launcher by finite elements method," *Gazi Üniversitesi Mühendislik-Mimarlik Fakültesi Dergisi*, vol. 30, no. 4, pp. 605–614, Dec. 2015. [Online]. Available: https://dergipark.org.tr/tr/pub/gazimmfd/issue/26692/280789

[25] F. Daldaban and V. Sari, "The optimization of a projectile from a three-coil reluctance launcher," *TURKISH J. Electr. Eng. Comput. Sci.*, vol. 24, pp. 2771–2788, 2016, doi: 10.3906/elk-1404-18.

[26] V. Sari and F. Daldaban, "Examination of the effect of different projectile geometries on the performance of reluctance launcher using 3D finite element analysis," *Cumhuriyet Sci. J.*, vol. 40, no. 2, pp. 518–526, Apr. 2019, doi: 10.17776/csj.392910.

[27] L. M. Cooper, A. R. Van Cleef, B. T. Bristoll, and P. A. Bartlett, "Reluctance accelerator efficiency optimization via pulse shaping," *IEEE Access*, vol. 2, pp. 1143–1148, 2014, doi: 10.1109/ACCESS.2014.2359996.

[28] H. Chen, R. Nie, M. Sun, W. Deng, and K. Liang, "3-D electromagnetic analysis of single-phase tubular switched reluctance linear launcher," *IEEE Trans. Plasma Sci.*, vol. 45, no. 7, pp. 1553–1560, Jul. 2017, doi: 10.1109/TPS.2017.2706195.

[29] M. Coramik, H. Citak, S. Bicakci, H. Gunes, Y. Aydin, and Y. Ege, "Studies to increase barrel exit velocity for four-stage coil-gun," *IEEE Trans. Plasma Sci.*, vol. 48, no. 7, pp. 2618–2627, Jul. 2020, doi: 10.1109/TPS.2020.2999110.

[30] Y. Hu, Y. Wang, Z. Yan, M. Jiang, and L. Liang, "Experiment and analysis on the new structure of the coilgun with stepped coil winding," *IEEE Trans. Plasma Sci.*, vol. 46, no. 6, pp. 2170–2174, Jun. 2018, doi: 10.1109/TPS.2018.2837089.

[31] H. Chen, Z. Li, W. Yan, and R. Nie, "Flux characteristics analysis of a single-phase tubular switched reluctance linear launcher based on 3-D magnetic equivalent circuit," *IEEE Trans. Plasma Sci.*, vol. 47, no. 5, pp. 2507–2513, May 2019, doi: 10.1109/TPS.2019.2903138.

[32] H. Chen, W. Yan, and Z. Li, "Flux characteristics analysis of a single-phase tubular switched reluctance linear launcher," *IEEE Trans. Plasma Sci.*, vol. 47, no. 5, pp. 2316–2322, May 2019, doi: 10.1109/TPS.2019.2895841.

[33] A. Mosallanejad and A. Shoulaie, "A novel structure to enhance magnetic force and velocity in tubular linear reluctance motor," *Turkish J. Electr. Eng. Comput. Sci.*, pp. 1063–1076, Jan. 2012, doi: 10.3906/elk-1012-953.

[34] J. Zhao, H. Li, B. Zhao, J. Liu, L. Kong, and P. Zhang, "An improved pulsed power supply circuit for reluctance electromagnetic launcher based on bridge-type capacitor circuit," *IEEE Trans. Plasma Sci.*, vol. 51, no. 5, pp. 1351–1356, May 2023, doi: 10.1109/TPS.2023.3265933.

[35] Z. Chaowei, D. Pengshu, D. Xiaojun, L. Sanqun, L. Zhiyuan, and Z. Guanghui, "Analysis of reluctance coil launcher performance using coupled field-circuit method," in *Proc. Int. Conf. Electr. Mach. Syst.*, Wuhan, China, 2009, pp. 4049–4052.

[36] *ON Semiconductor Corporation, Application Note 9020, IGBT Basic II*. Accessed: Aug. 18, 2023. [Online]. Available: https://www.onsemi.com/pub/collateral/an-9020.pdf

[37] Infineon Technologies. *IR2113 High and Low Side Driver Datasheet*. Accessed: Aug. 18, 2023. [Online]. Available: https://www.infineon.com/dgdl/Infineon-IR2110-DataSheet-v01_00-EN.pdf?fileId=5546d462533600a4015355c80333167e

VEKIL SARI received the B.Sc. degree in electrical and electronics engineering from Karadeniz Technical University, Turkey, in 1997, the M.Sc. degree in electrical and electronics engineering from Hacettepe University, Turkey, in 2002, and the Ph.D. degree in electrical and electronics engineering from Erciyes University, Turkey, in 2015.

Since 2015, he has been an Assistant Professor with the Department of Electrical and Electronics Engineering, Faculty of Engineering, Sivas Cumhuriyet University. His research interests include the design of electrical machines, electromagnetic launchers, and renewable energy.